Spin Filters for Spintronic Logic Devices

NRI-NSF project
Annual review presentation

Dipanjan Mazumdar
MINT Center, University of Alabama

September 9th 2010

People Involved

Post Docs: Dipanjan Mazumdar, Vijay Kartik and Jianxing Ma

Graduate Students: Xing Zhong, Hunter Sims, Manjit Pathak

Faculty: Arunava Gupta, Patrick Leclair, Bill Butler, Su Gupta, Tim Mewes

Collaborators

Polarized Raman Spectroscopy
Milko Iliev, Texas Center for Superconductivity and Advanced Materials

Depth-resolved Cathodoluminescence Spectroscopy
Shaopin Shen and Leonard J. Brillson, Ohio State University

High Resolution Transmission Electron Microscopy
Ranjan Dutta, Jawaharlal Nehru Centre for Advanced Scientific Research, India

Publications relevant to this work…

1. A Robust Approach for the Growth of Epitaxial Spinel Ferrite Films, JAP (2010), (*in press)*
2. Formation of antiphase domains in $NiFe_2O_4$ thin films deposited on different substrates, APL 97, 071907 (2010)
3. Monitoring B-site ordering and strain relaxation in NiFe2O4 epitaxial films by polarized Raman spectroscopy (submitted to PRB)

and a couple more in progress…

Spintronics (Spin-Electronics)

- **Devices which are sensitive to the electronic spin degree of freedom**
- **Devices showing the *magnetoresistance* effect constitutes the most mature area of spintronics**
- **Many material candidates exist capable of showing the MR effect**
- **Emphasis on room-temperature applications**
- **Easy manipulation of magnetotransport properties by an external magnetic field or current**

Outline

1) **Part 1- Overview of MR devices**

a) **GMR and TMR devices**
b) **Spin filter devices**

2) **Part 2 - Materials and Characterization**

a) **Magnetic Insulators**
b) **Film growth, Raman, TEM, Cathodoluminense, Device fabrication**

3) **Part 3 - Theory**

Progress in *Ab-initio* techniques to estimate band-gap

Giant Magnetoresistance - GMR (1988)

First observed in Fe/Cr multilayers (FM/M/FM)

$$MR = \frac{\Delta R}{R_{\uparrow\uparrow}} = \frac{R_{\uparrow\downarrow} - R_{\uparrow\uparrow}}{R_{\uparrow\uparrow}} \sim 20\ \%\ \text{at RT}$$

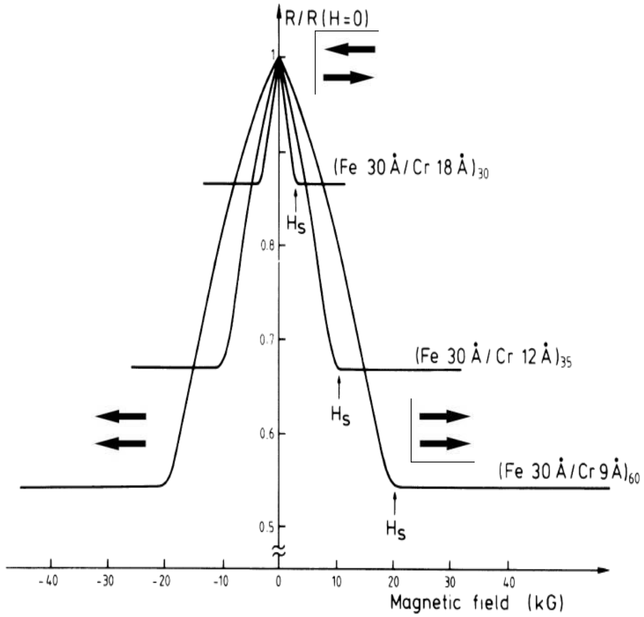

Two Resistor Model

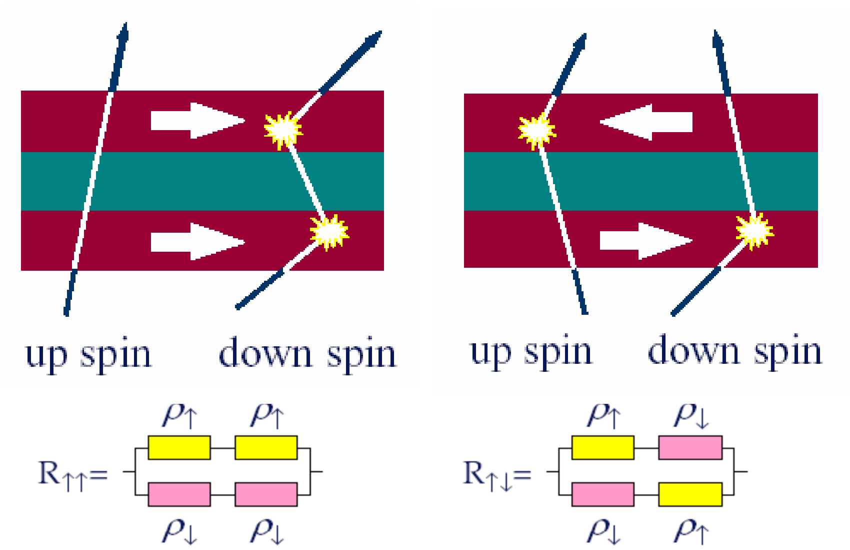

Baibich *et. al.* PRL (1988)

2007 Physics Noble Prize, A. Fert and P. Grunberg

Magnetic Tunnel Junction (FM/I/FM)

First observed by Julliere in 1975 in Fe/Ge/Co trilayer, MR~14% at 4.2K.

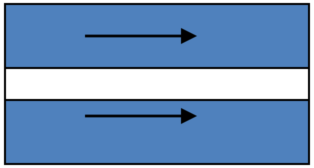

Julliere Model

$$\text{TMR} = \frac{2P_1P_2}{1-P_1P_2}$$

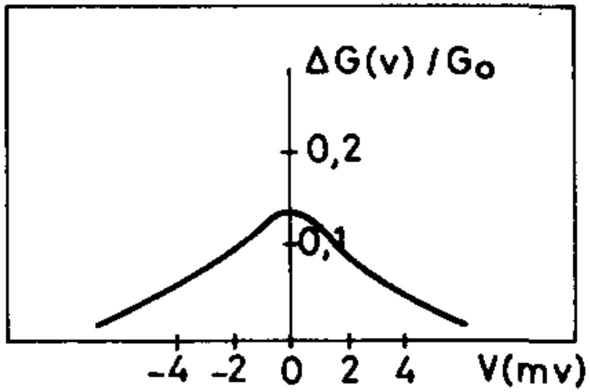

P_1, P_2 are spin polarizations of two FM materials

$$P_{1(2)} = \frac{D^{\uparrow}_{1(2)} - D^{\downarrow}_{1(2)}}{D^{\uparrow}_{1(2)} + D^{\downarrow}_{1(2)}}$$

No Room temperature effect seen by Julliere. Results never reproduced.

Physics Letters A 54(3): p. 225-226 1975

Magnetic Tunnel Junction (cont.)

In 1995, substantial RT MR (>10%) was observed by Moodera (MIT) and Miyazaki (Japan)

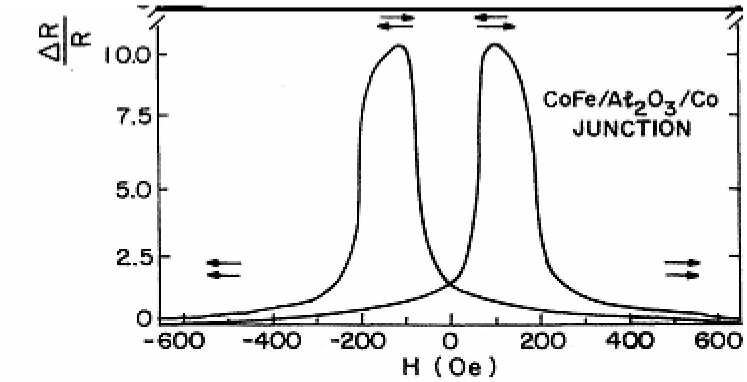

Until 2004, 20-70 % MR has been reported on Al_2O_3 based junctions

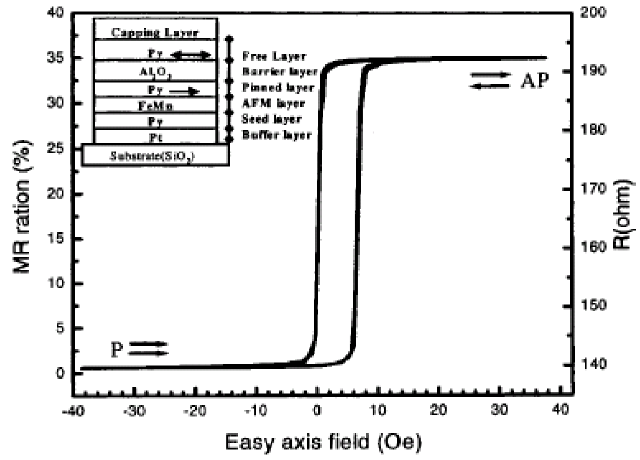

Using Julliere's formula,

TMR ~ 67% for P = 0.5

~ 20% for P= 0.3

Spin coherent Tunneling

- ***Symmetry***
- ***Decay of states within the barrier***
- ***Symmetry-filtering***

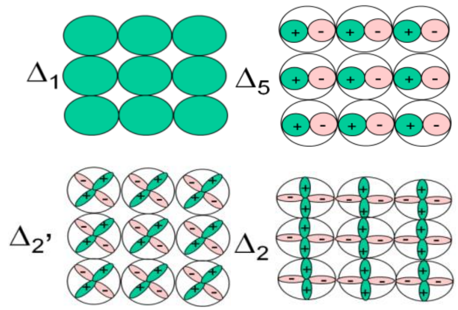

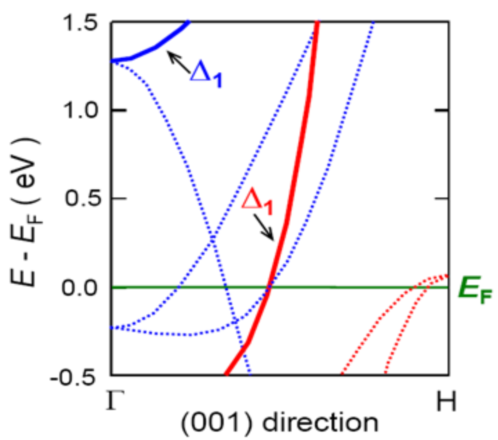

Fe band

majority spin
minority spin

Amorphous Al-O barrier

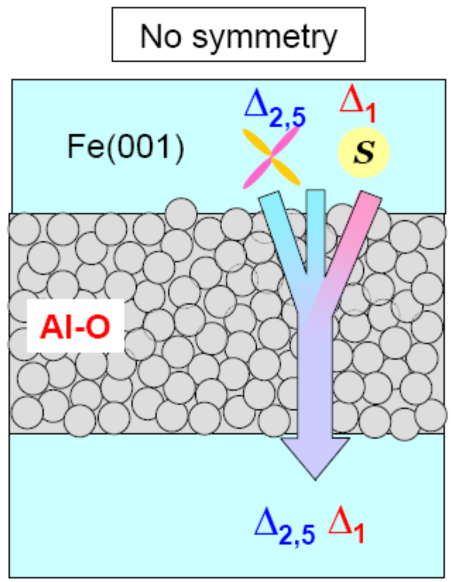

Incoherent tunneling

MgO(001) barrier

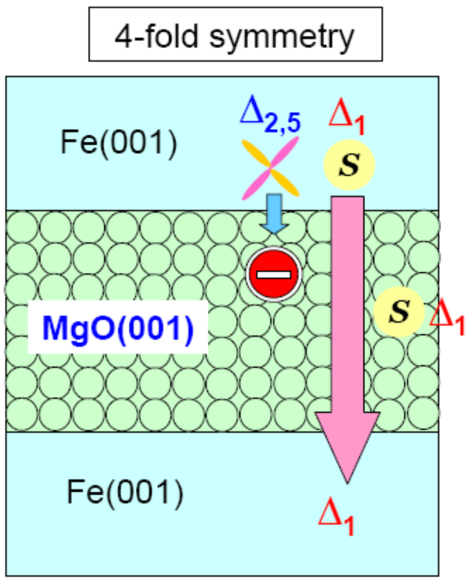

Coherent tunneling

Butler *et al* (2001) , Mathon *et al* (2001)

Spin coherent Tunneling (cont.)

For Fe, Co and CoFe there is no minority Δ_1 band at the Fermi level

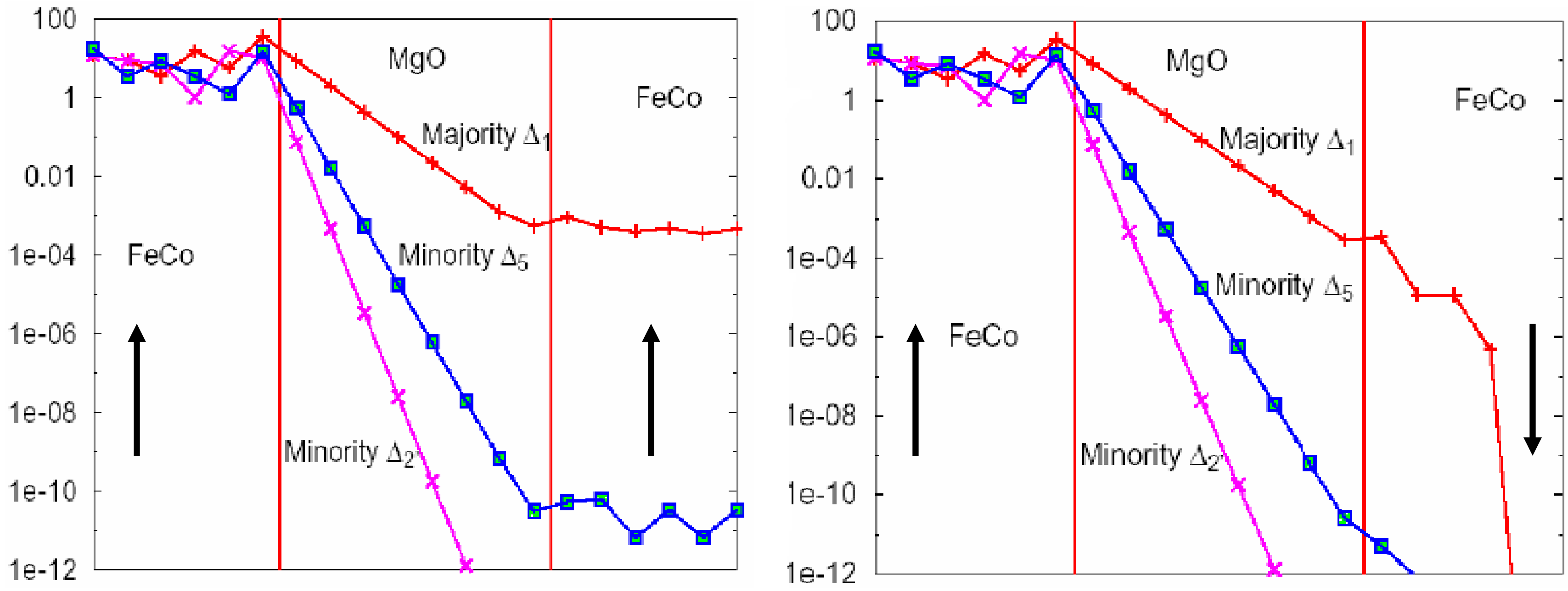

Zhang and Butler (2004)

First high MR realization

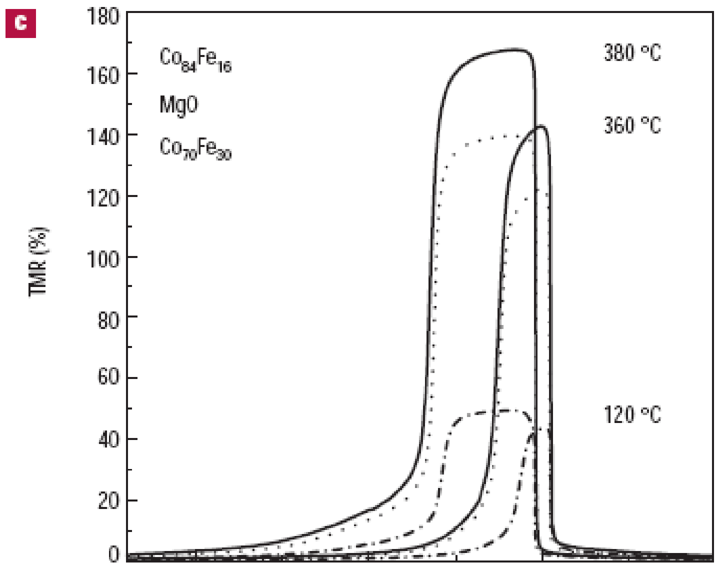

Parkin *et. al.* (2004), IBM

Spin polarization = 85%

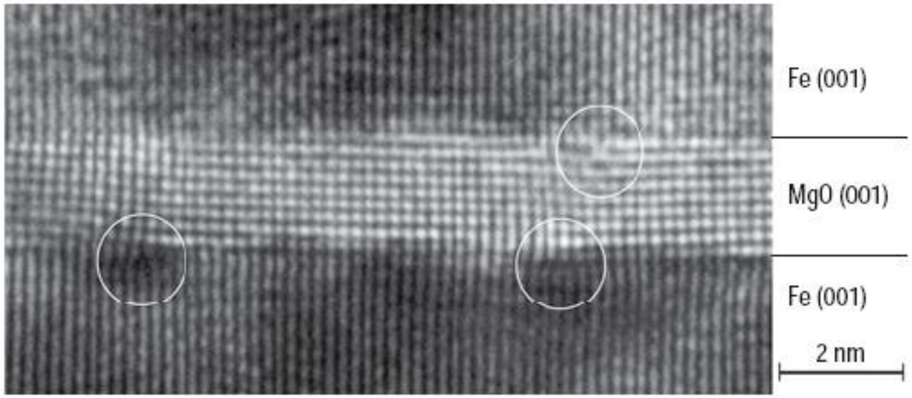

Yuasa *et. al.* 2004, AIST Japan

Current highest TMR at RT is over 600%

If the barrier is magnetic…

Spin filter devices …

Conceptually explored back in the 60s (Esaki, Stiles, Von Molnar)

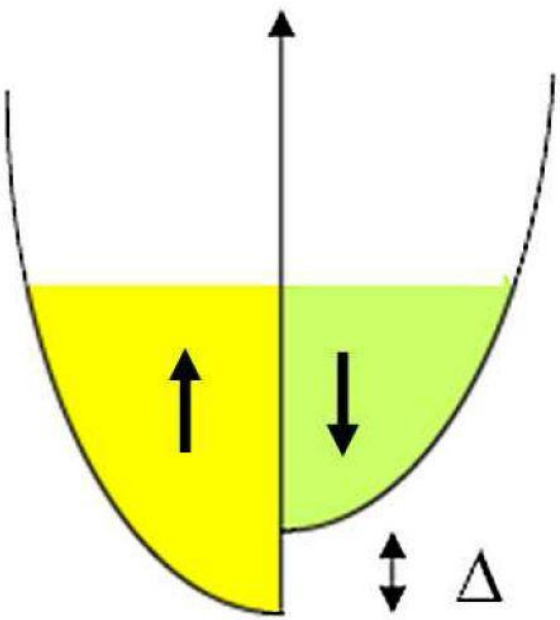

Stoner Model of Ferromagnetism

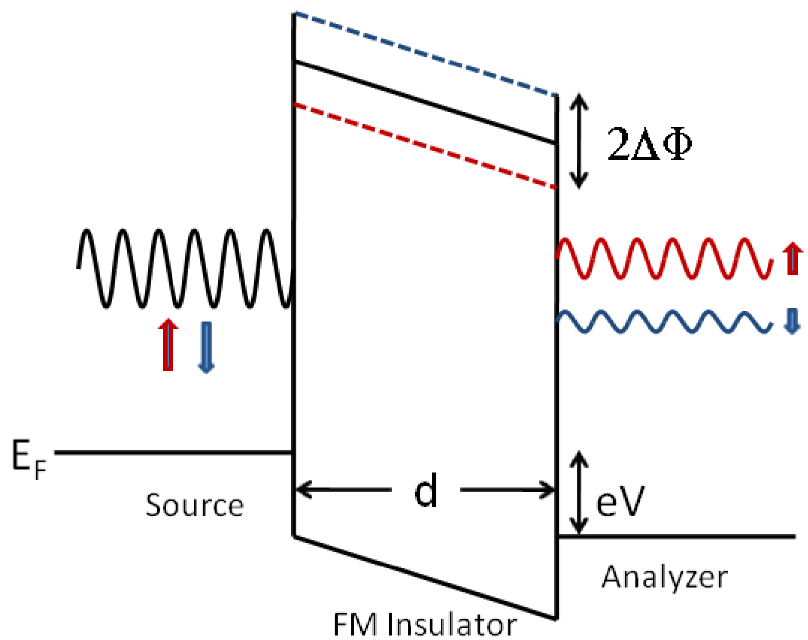

$2\Delta\Phi$ = 0.54 eV for EuO

Spin Filters (cont.)

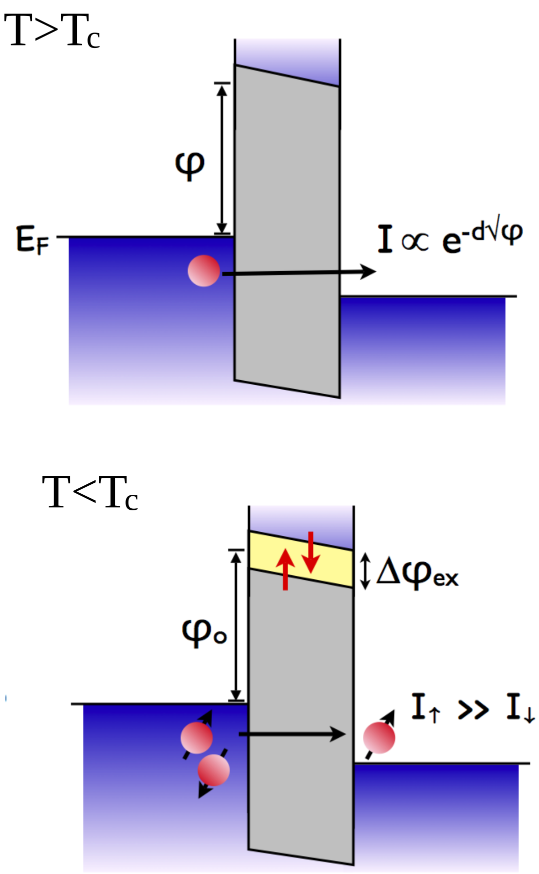

- Spin-dependent barrier height in FM insulator
- Spin filtering efficiency ~100% has been demonstrated at low temperatures
- MR >100% demonstrated at LT
- Small RT evidence with spinels
- Potentially, TMR ratios of over 10^5 with double spin filters (Worledge, APL 2000)

Early Work – Moodera et. al. (88), LeClair et. al. (02) on chalcogenides
Luders et. al. (06), Ramos et. al. (07) on spinel-ferrites
Gajek et. al. (06,07) on perovskites

First step: Spin filter + Magnetic electrode

- Spin filter - highly polarized current
  ferromagnet - spin analyzer

- Parallel magnetizations: low resistance

- Antiparallel magnetizations: high resistance

- Advantages?
  Spin filter efficiency is high

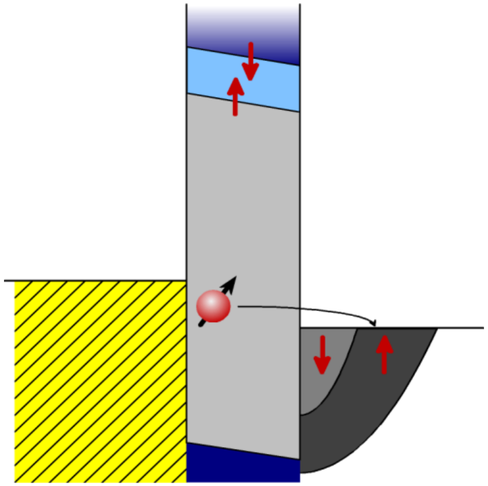

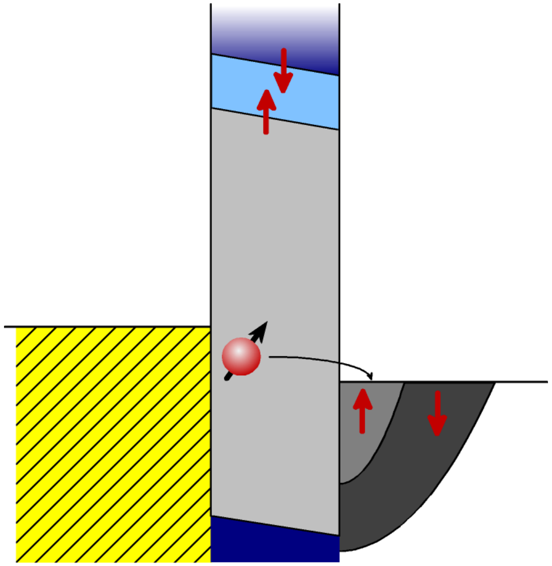

LeClair *et. al.* - 130% MR @ 5K - Al/EuS/Gd

Gajek *et. al.* - 50% MR - Au/$BiMnO_3$/LSMO

Double Spin filter…

If one filter is good ... two are better!

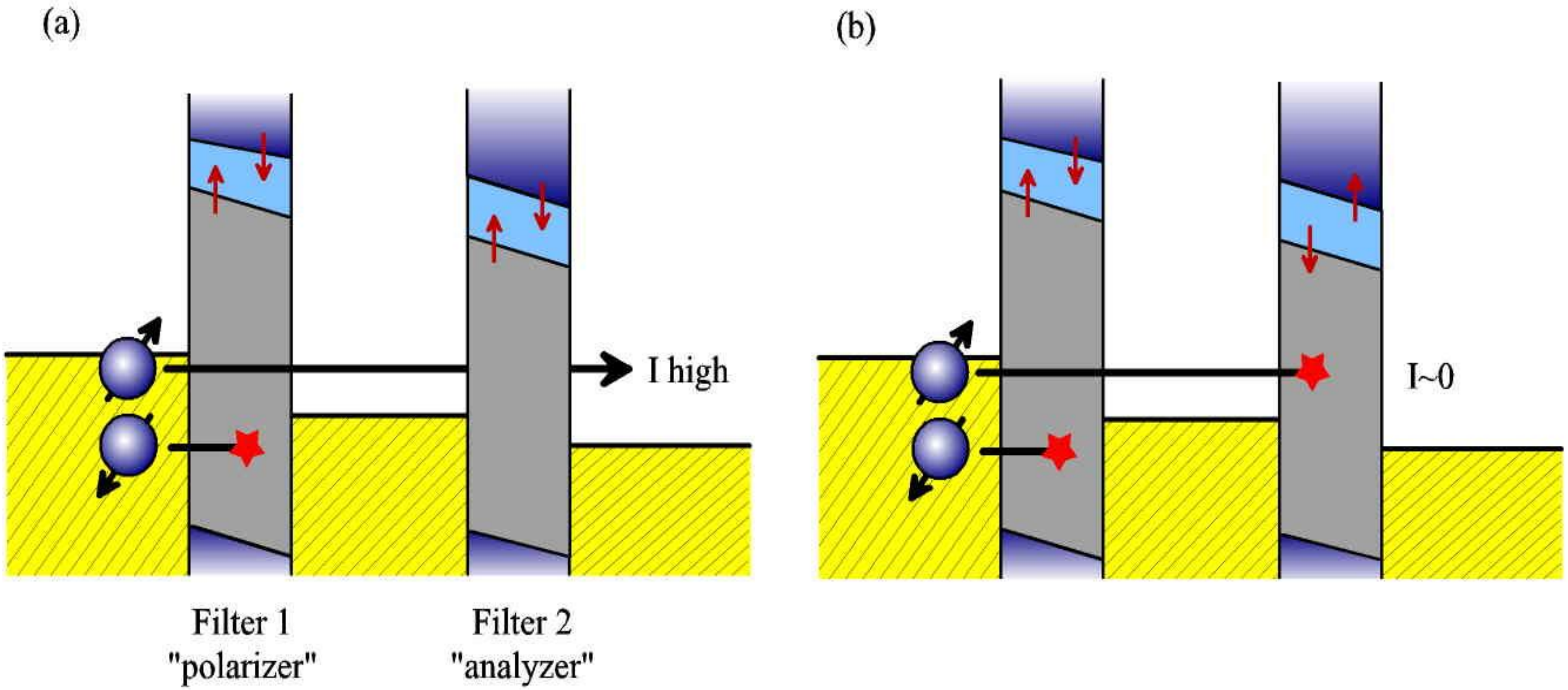

Functions like an optical polarizer/analyzer

Provides higher on/off ratio required for logic applications

Up to 10^5 MR ratio predicted (Worledge)

Part 2 – Materials and Characterization

Materials - Magnetic Insulators with High Tc

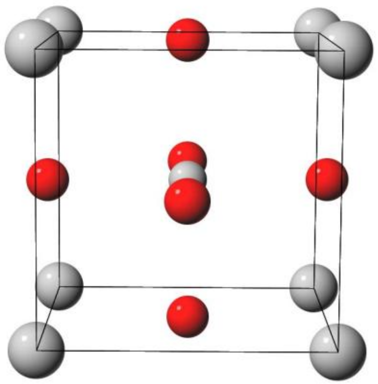

Perovskite (ABO_3)

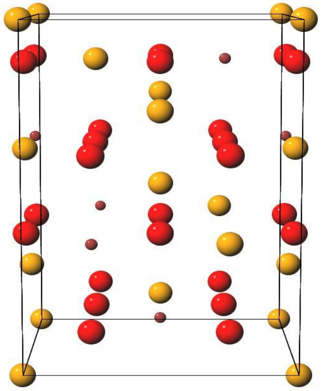

Spinel (AB_2O_4)

Oxide Family	Conducting & Magnetic	Insulating & Magnetic		Conducting or Insulating & Non-Magnetic
		material	*magnetism type, T_C (K)*	*oxides/metals*
Single and Double Perovskites	$La_{1-x}Sr_xMnO_3$ x = 0.3-0.4, FM, T_C ~ 360 K	La_2NiMnO_6	FM, 287	***Conducting*** $LaNiO_3$,[1] $CaRuO_3$,[1] $SrRuO_3$ > 160K, Nb:$SrTiO_3$ ***Insulating*** $SrTiO_3$, $LaAlO_3$, $NdGaO_3$, $LaMnO_3$[2]
		La_2CoMnO_6	FM, 233	
		Bi_2CuMnO_6	FM, 340	
	Ca_2FeMoO_6, Sr_2FeMoO_6, Sr_2CrReO_6, FM T_C ~ 365, 420, 635 K	Ca_2CrReO_6	FRI, 360	
		Ca_2FeReO_6	FRI, 525	
Spinels	Fe_3O_4, FRI T_C ~ 600 K	$NiFe_2O_4$	FRI, 850	***Conducting*** (TiN, Pt) ***Insulating*** $MgAl_2O_4$
		$CoFe_2O_4$	FRI, 795	

FM: Ferromagnetic; FRI: Ferrimagnetic
[1] PM: Paramagnetic Metal; [2] AF: Antiferromagnetic Insulator

Spinels

General Formula – AB_2O_4

- Fcc oxygen lattice
- 12.5% tetrahedral and 50% octahedral sites occupied
- A and B are cations with valence +2 or +3

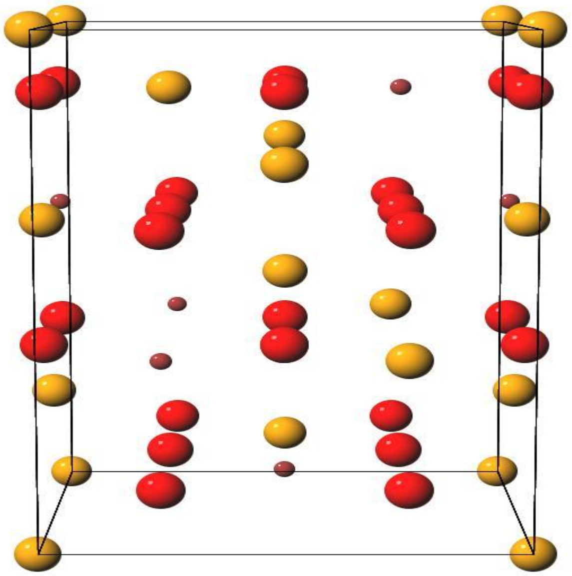

Spinel (AB_2O_4)

Normal and Inverse Spinel

Normal – $(A)_{tet}\ (BB)_{oct}$

Inverse – $(B)_{tet}\ (BA)_{oct}$

Spinels (cont.) – Problem of cation ordering

- **Bulk NFO and CFO orders in the inverse spinel structure**

- **Magnetically , it is a ferrimagnetic system. The Fe sublattice aligns anti-ferromagnetically. Resultant magnetic moment is from Ni^{2+} (Co^{2+}) ion for NFO (CFO).**

- **Magnetic moment of 2μB/fu for NFO and 3μB/fu for CFO**

- **Exchange interactions are mediated by O^{2-} ions (superexchange interaction).**

<u>Growth requirements</u>

High quality epitaxial thin films , defect free, with bulk magnetization preserved down to unit cell level.

Pulsed Laser Deposition (PLD) of Oxide Materials

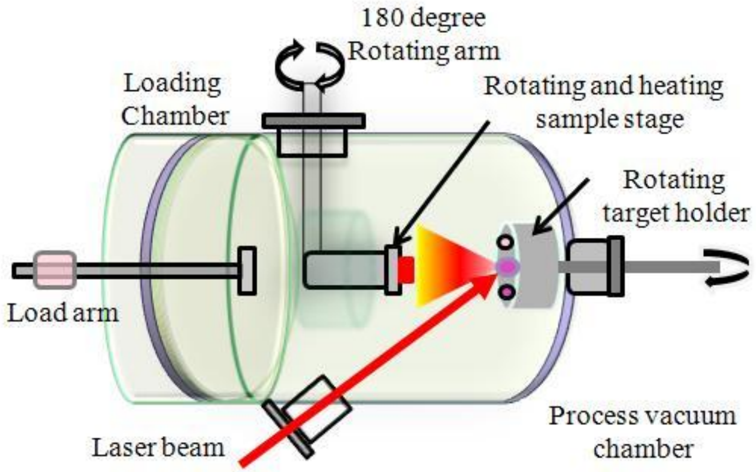

Two PLD chambers

KrF excimer laser source ~ 248 nm
Max. temperature – 750 C
In-situ RHEED monitoring.

UA Characterization Facilities

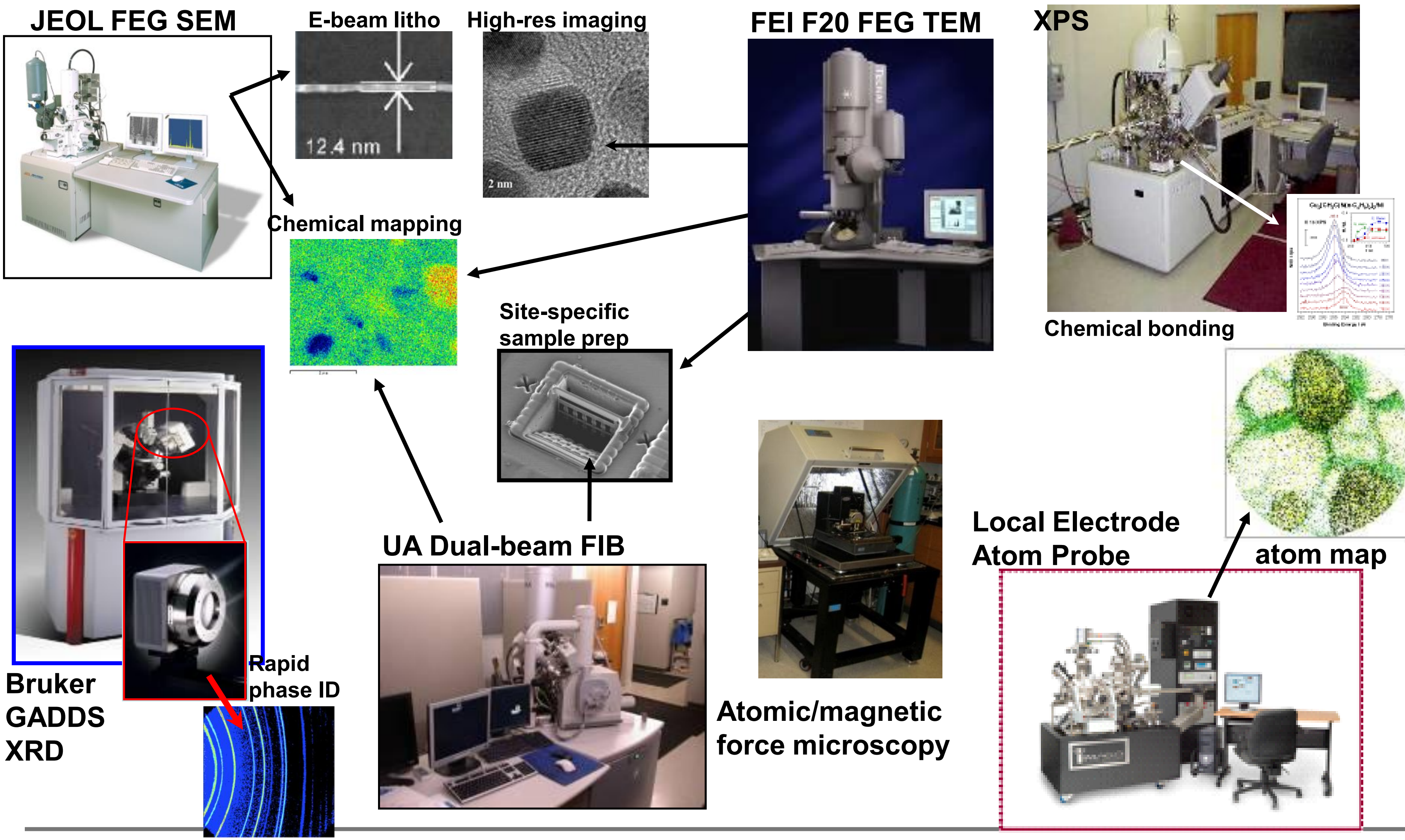

Growth of high quality epitaxial NFO and CFO thin films

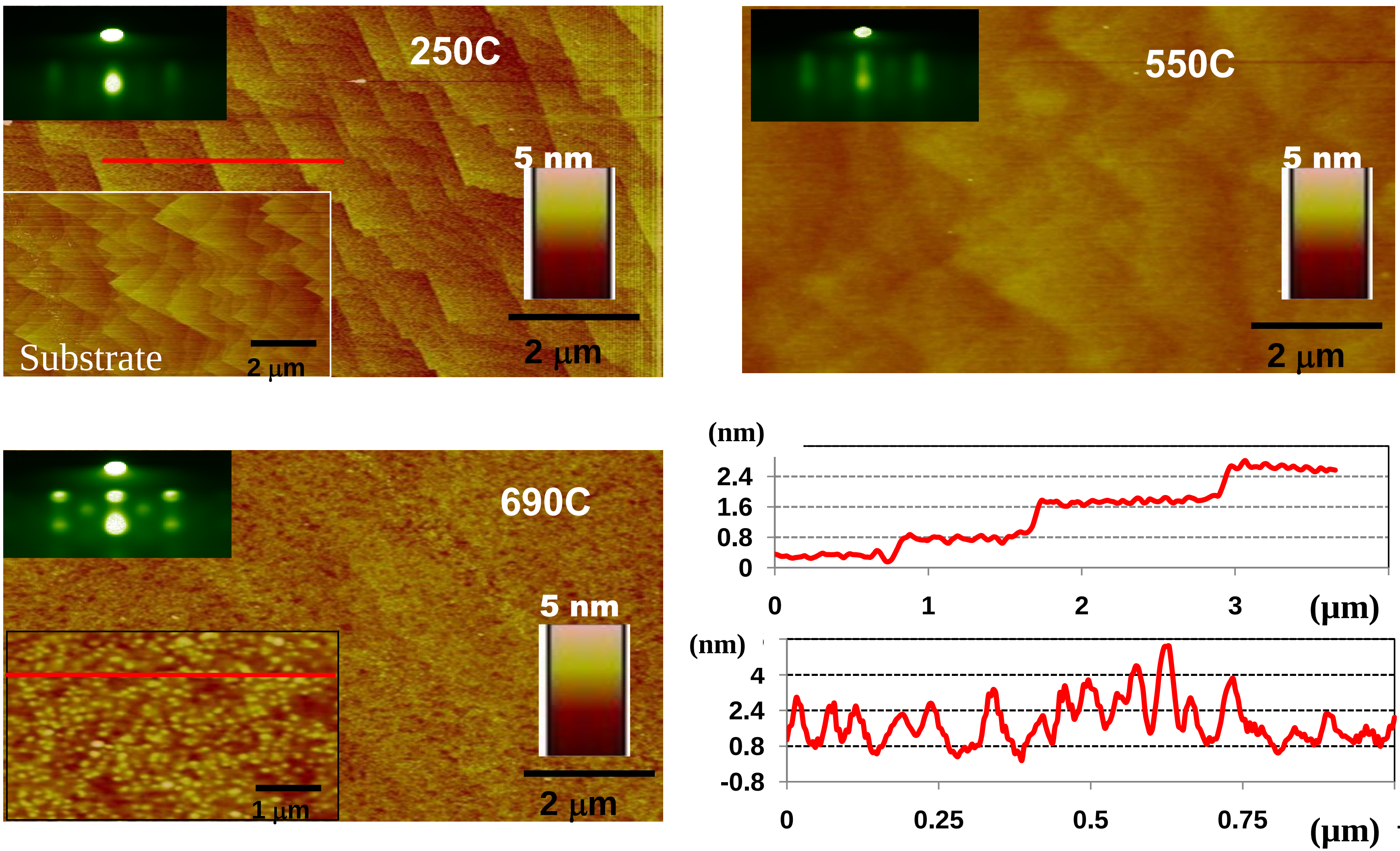

220 nm film thickness

Journal of Applied Physics (2010)

Structural Characterization (cont.)

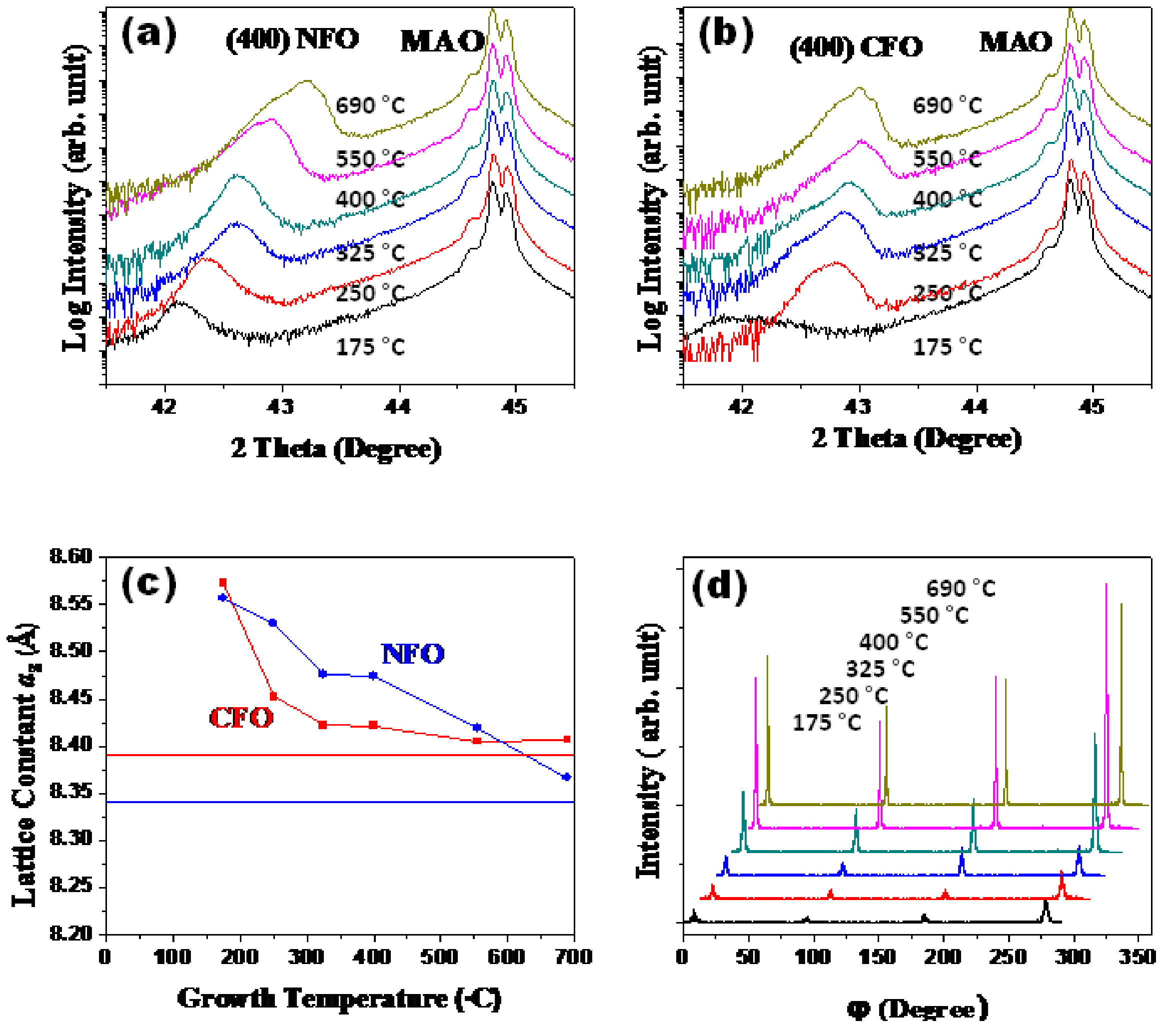

Journal of Applied Physics (2010)

Magnetic characterization

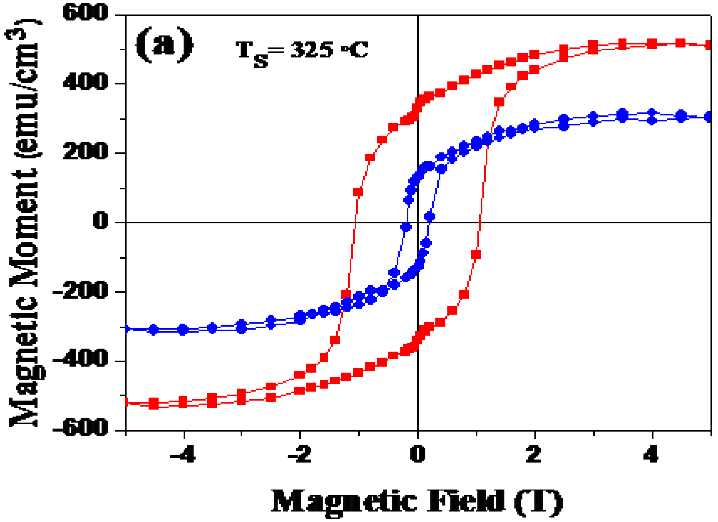

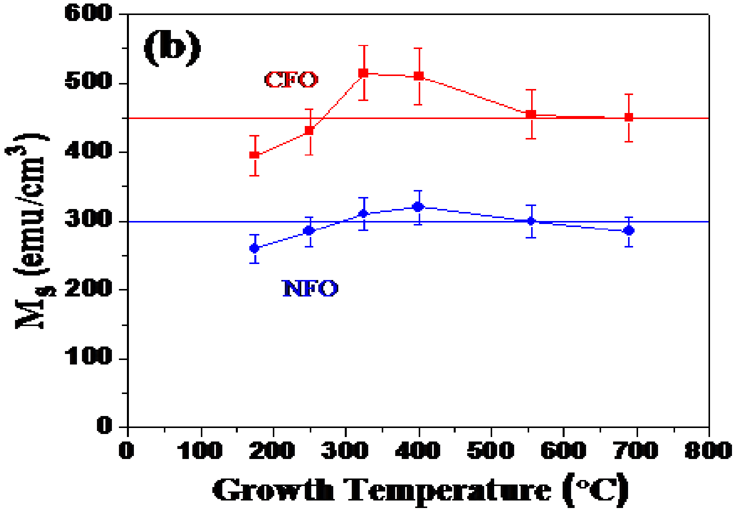

Polarized Raman Spectroscopy Investigations

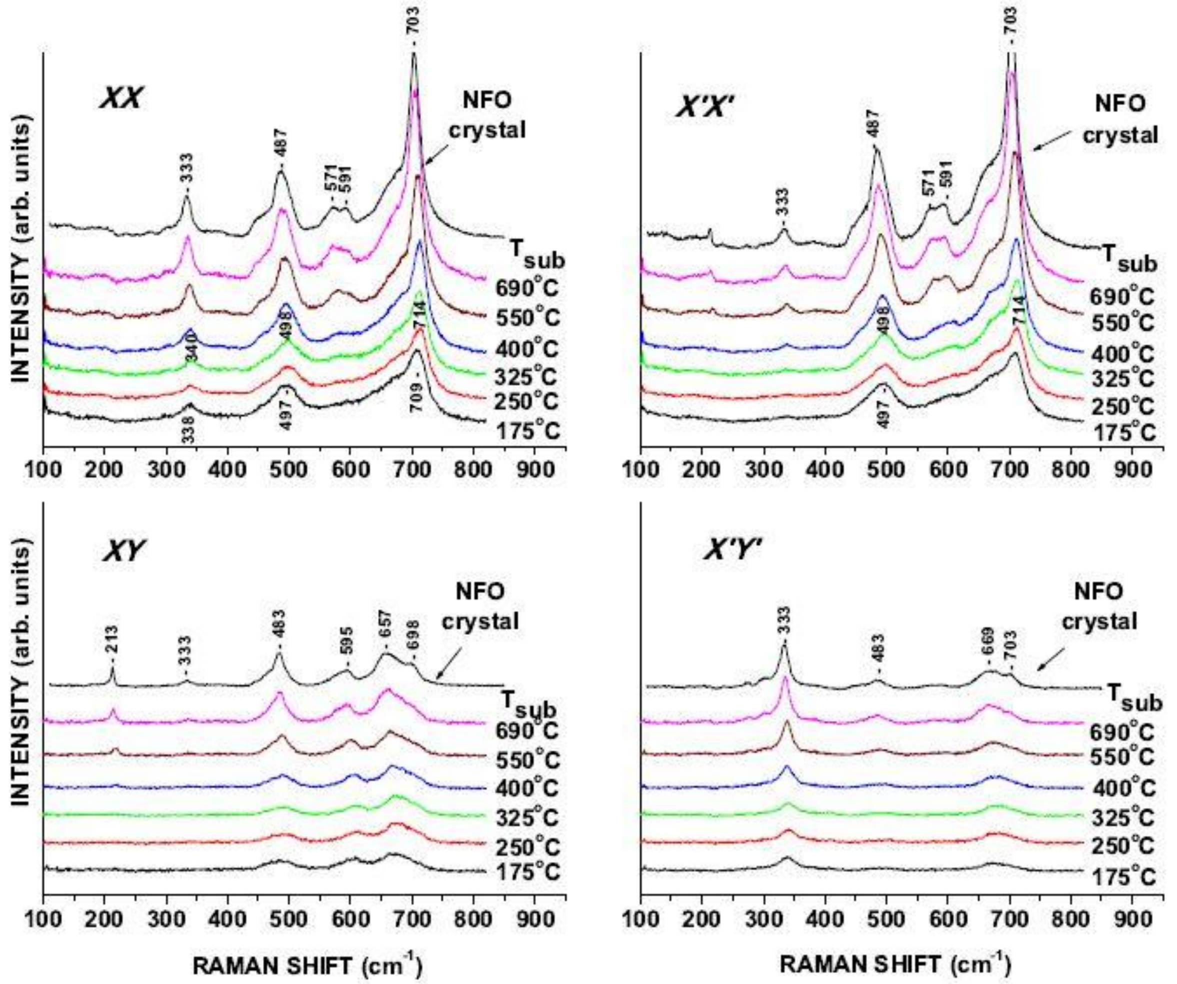

Polarized Raman Spectroscopy (cont.)

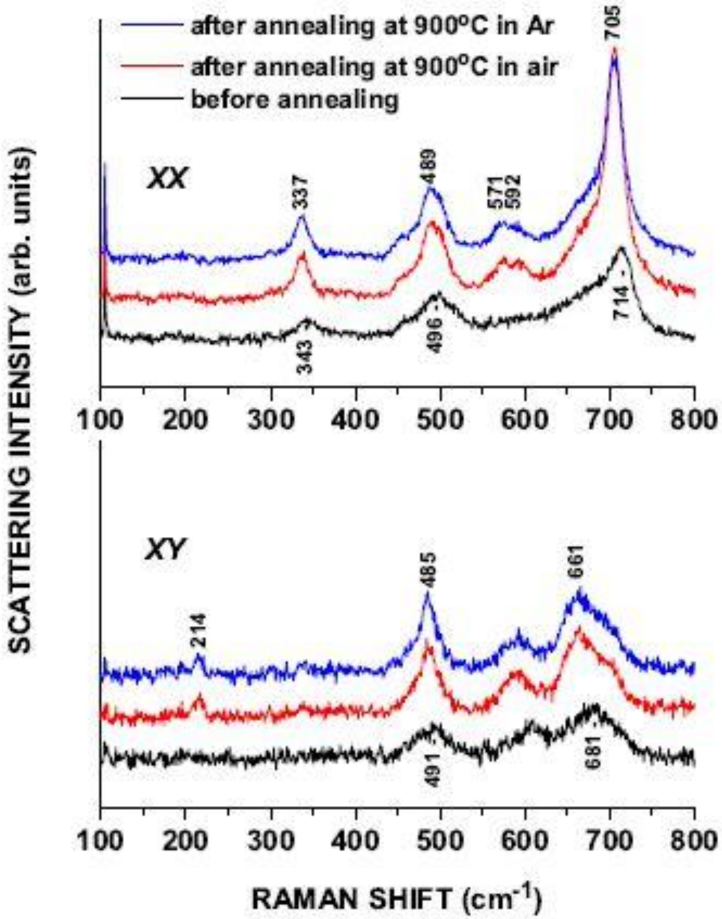

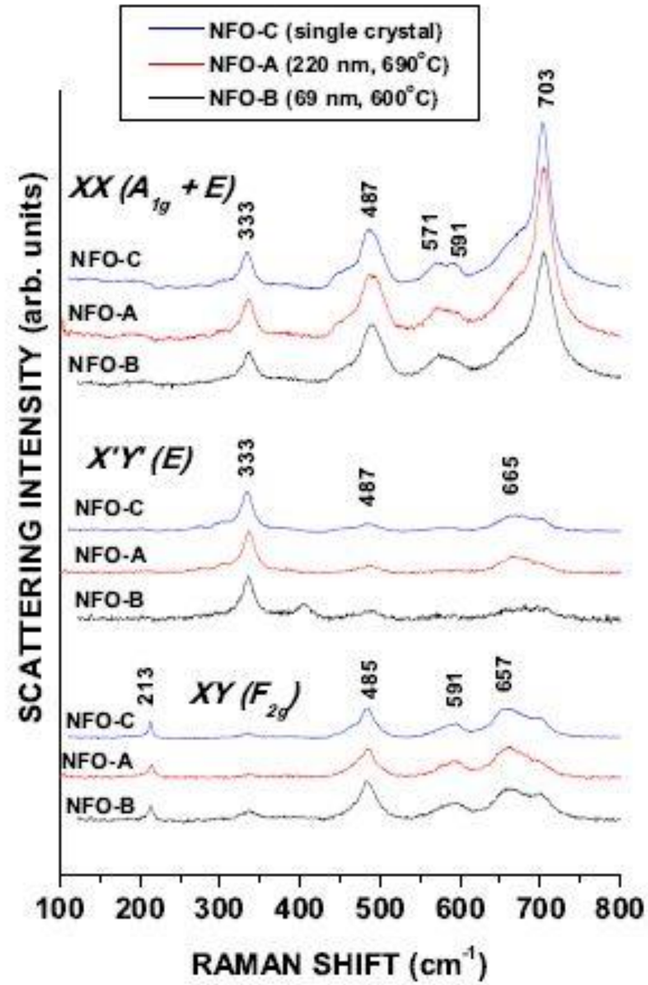

Sputtered samples (NFO-B) from Group of J. Fontcuberta (Spain)

Transmission electron microscopy analysis

<u>**Formation of Anti-phase boundaries**</u>

- **Large spinel unit cell**
- **Many inequivalent nucleation sites**
- **Could lead to anti-ferromagnetic coupling**

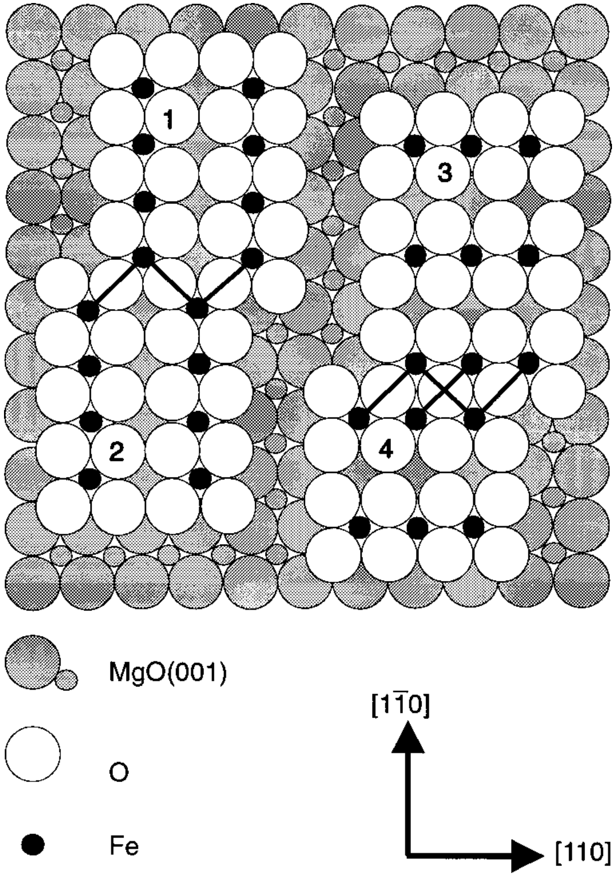

PRB 57 R8107 (1999)

Cross section TEM

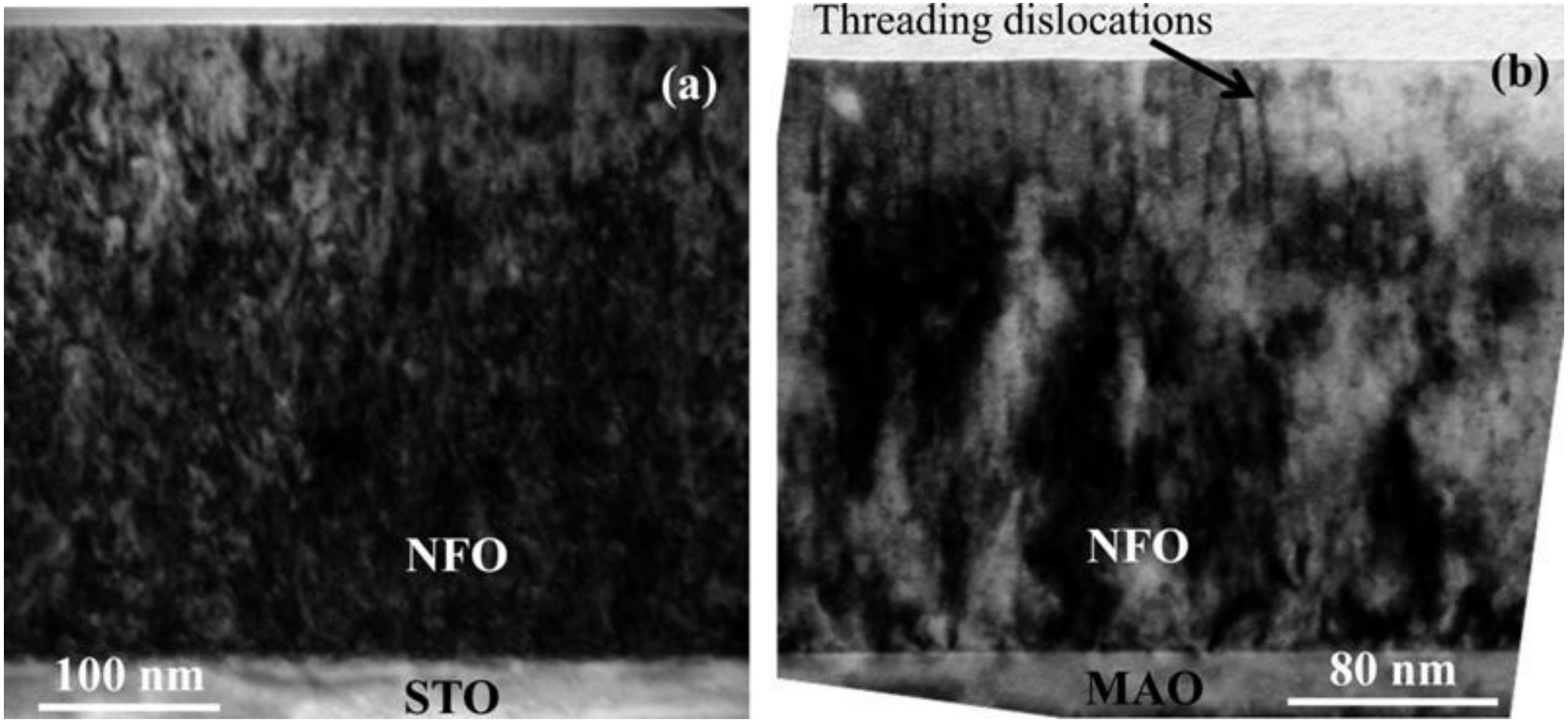

Anti-phase boundaries observed in all films grown at various temperatures

Plan-view TEM

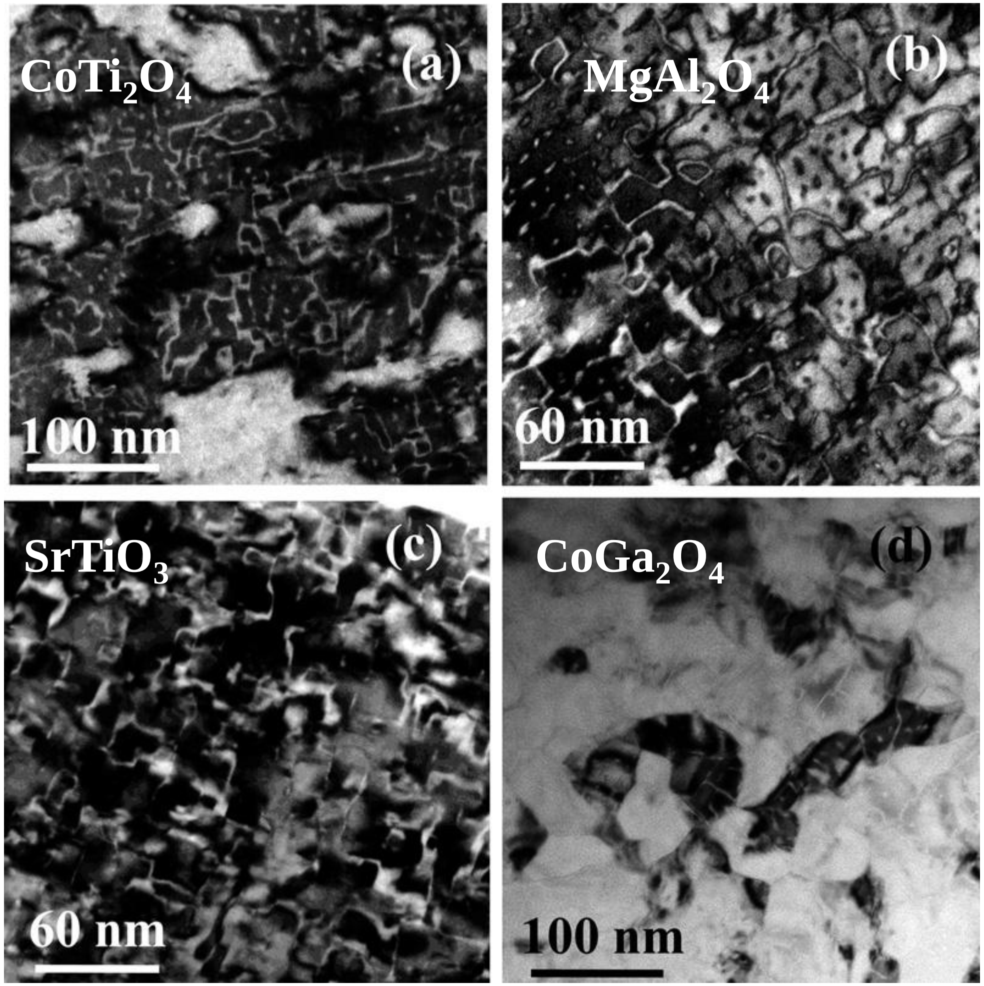

(APL 2010)

Qualitative estimates show low APB density for small lattice mismatch

High-resolution TEM

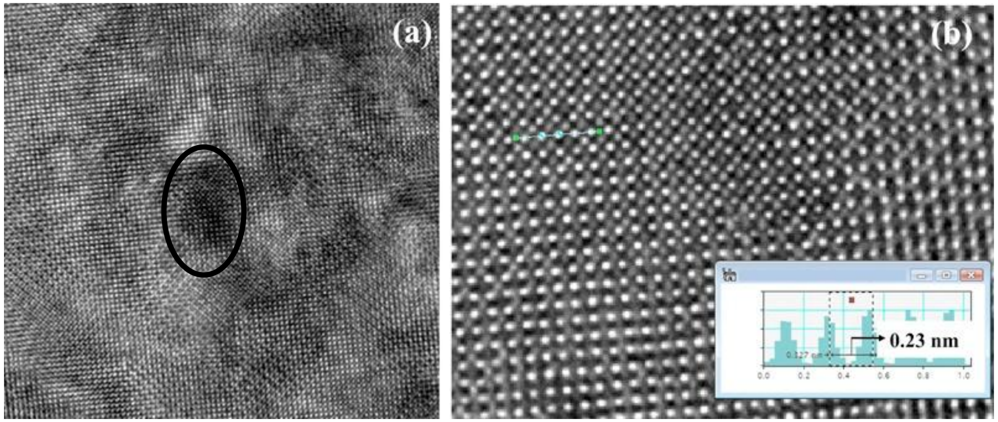

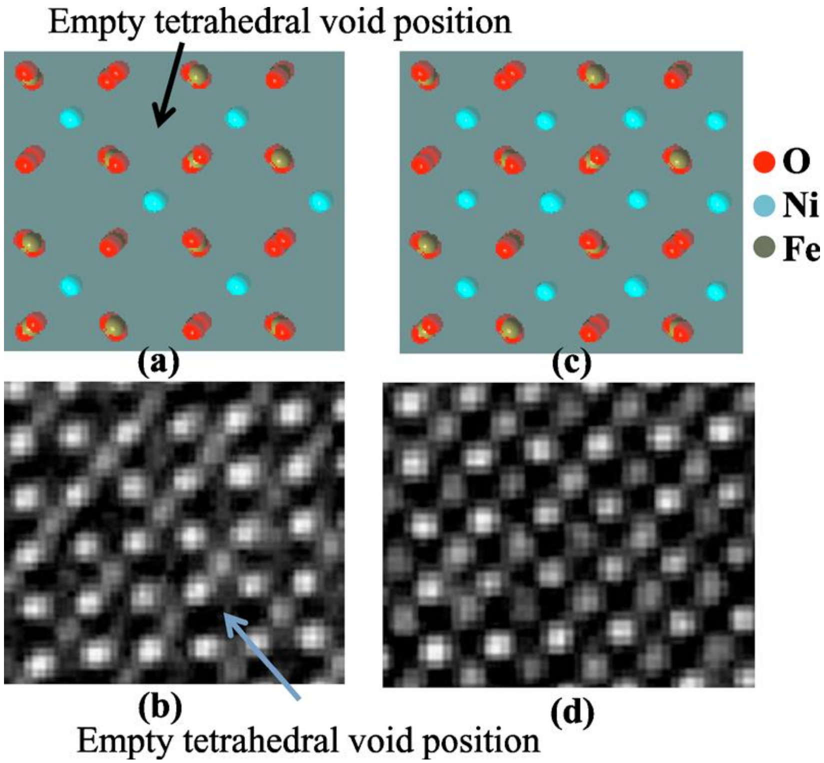

Dark diffuse regions indicate APBs

Occupation of interstitial tetrahedral sites

Cathodoluminescence Spectroscopy

- CL is defined as the emission of light (200 nm to 2500 nm) produced by electron irradiation
- When the electron and hole recombine, the ruptured chemical bond is restored, releasing its excess energy by the emission of an optical photon
- The DRCLS technique is capable of probing band gap and deep level defect features

Cathodoluminescence Spectroscopy Measurements

- $NiFe_2O_4$ spinel ferrite films grown on $MgAl_2O_4$(100) substrates with ozone-assisted PLD

- Two series of samples:
  1. As-grown 325ºC; As-grown 550ºC
  2. As-grown 325ºC; Annealed in O_2 at 550 ºC; and 700 ºC

- Two different CL measurements:
  1. 80K CL chamber 1 (high current, less charging, large beam radius good for bulk information, lens luminesecnce)
  2. 12K in SEM chamber (no lens luminesecnce, low temperature, severe charging, small beam radius-localized information)

- Sample thicknesses: approx. 220 nm ~250 nm

CL Measurements (cont.)

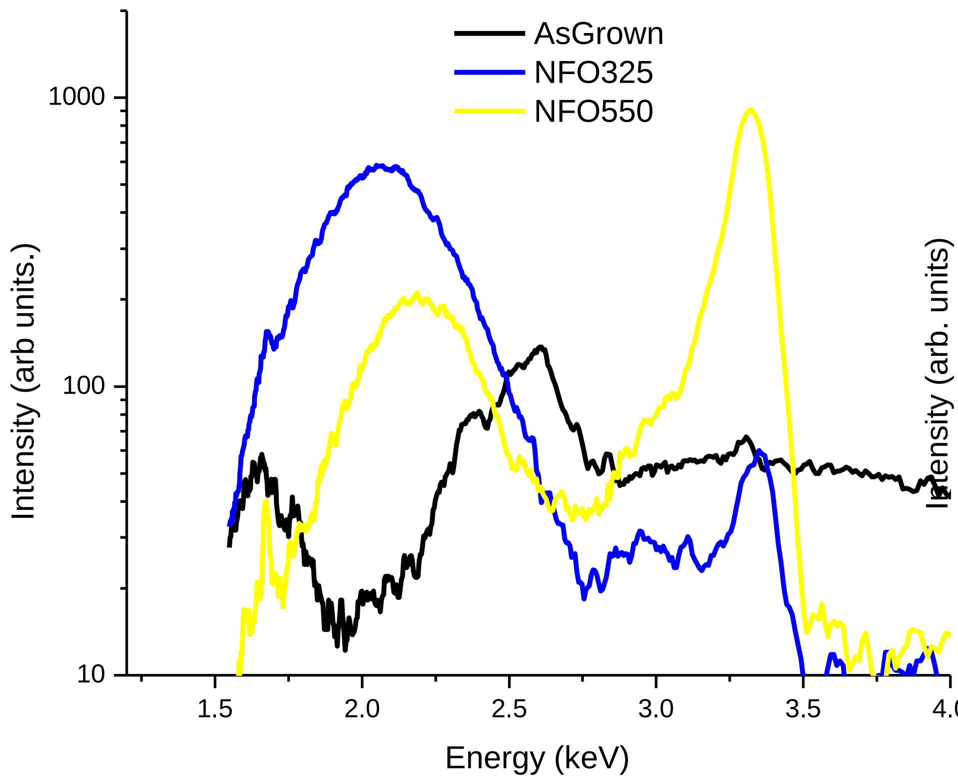

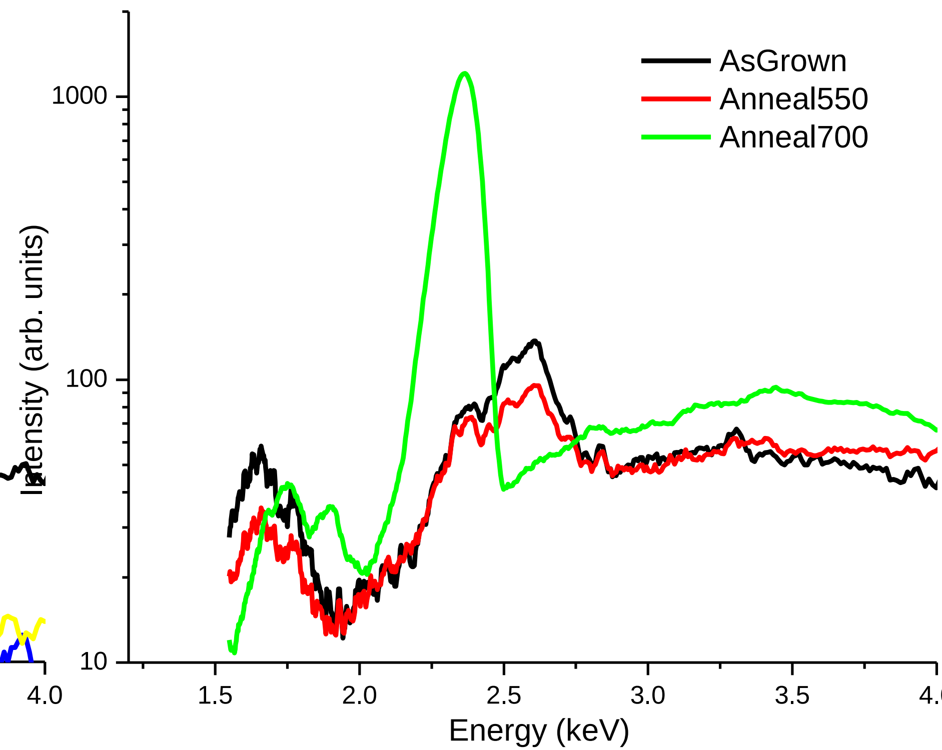

All As-Grown samples:

- **Higher growth Temperature, better defined impurity peaks and band gap emission**

Same sample different annealing:

- **Higher annealing T, strong 2.36 eV peak**
- **All suppressed E_g peak**
- **Again low T (550ºC) annealing change very little of the CL spectra**

Peak Origins Analysis

- 3.32 eV peak from SEM & ~3.4 eV shoulder from chamber 1 are essentially same, that is band gap of NFO
- 1.59 ev: Impurity frequently seen in complex oxide
- 1.67 eV: Probably due to second order emission of band gap
- 1.76 eV: NiO or Ni^{2+}
- 1.9 ~ 2.02 eV: $Fe^{3+}V$
- ~2.3 eV: might due to Fe^{4+}
- 2.3 ~ 2.4 eV: might also due to Ni ion
- Broad 2.4~2.5 eV deep level dominates emission: V_O-related
- 2.8 eV: $Fe^{4+}V$
- 2.8 ~3.05 eV: Ni ion

CL measurements summary

- **Best as-grown: 550ºC**
- **Best anneal: 550ºC**
- **Both samples show defect levels at similar energies: 1.76 eV, 2.45 eV and 3.15 eV**
- **Possible band gap emission around 3.35~3.4 eV depend on measurement temperature**
- **Defect levels identified:**
  Oxygen related: 1.59 and 2.5 eV
  Ni related: 1.76, 2.3~2.4, 2.8~3.05 eV
  Fe related: 1.9~2.02, 2.3, 2.8 eV

Spin filter device Prototype

FM/FI/Au

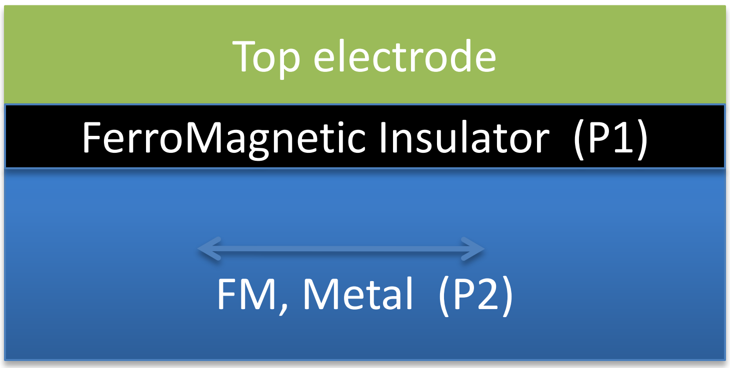

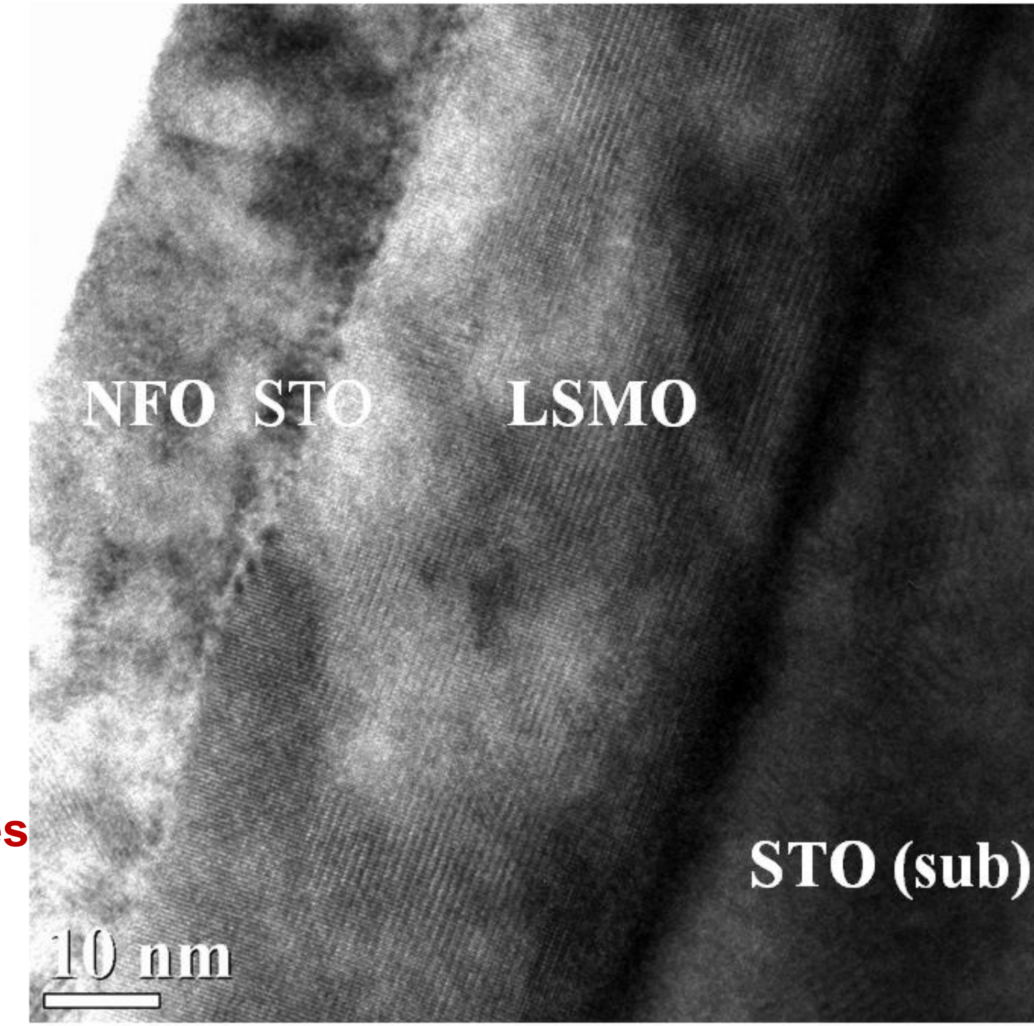

Thin non-magnetic layer decouples the magnetic layers

Device processing steps

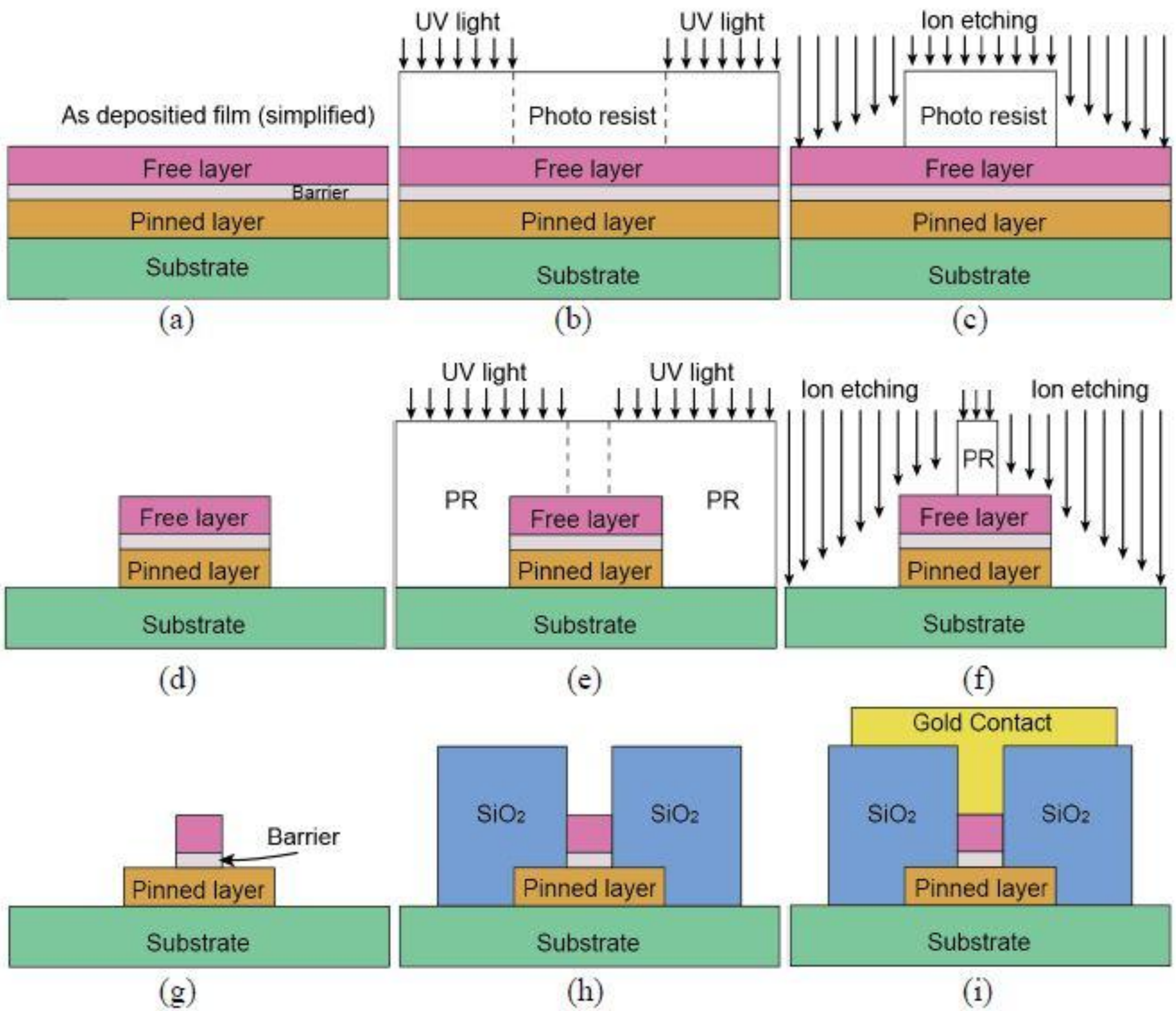

Microfabrication tools

Solitec photoresist spinner

Karl Suss mask aligner

Intelvac Ion mill

Denton Vacuum E-Beam Evaporator

STS Advanced Oxide Etcher (AOE)

Magnetotransport data @ 77K

LSMO (30)/STO(3)/NFO(3)/Au(100)

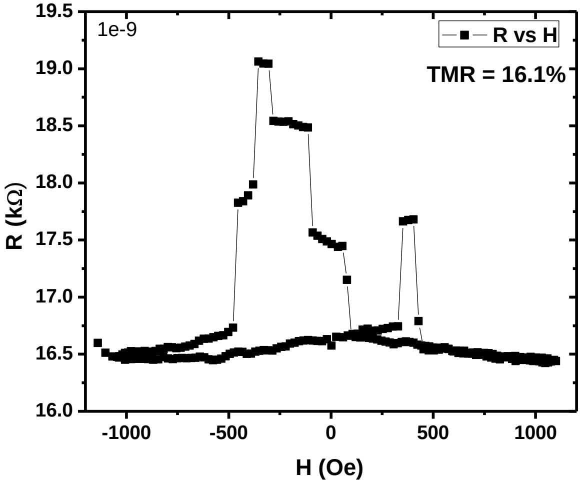

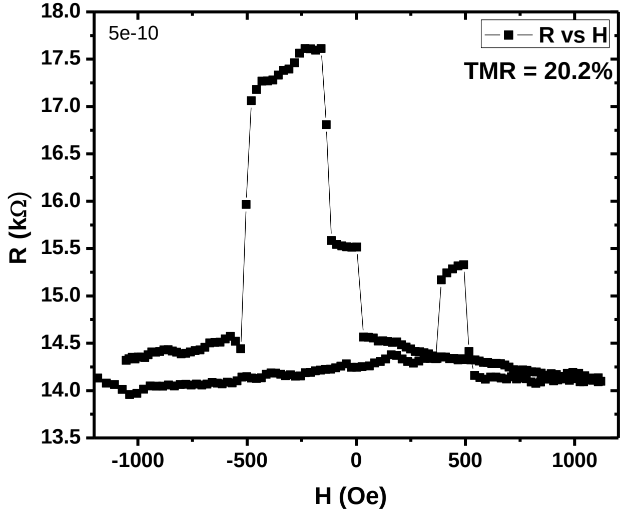

TMR showing normal bias voltage dependence

TMR value comparable with existing literature reports

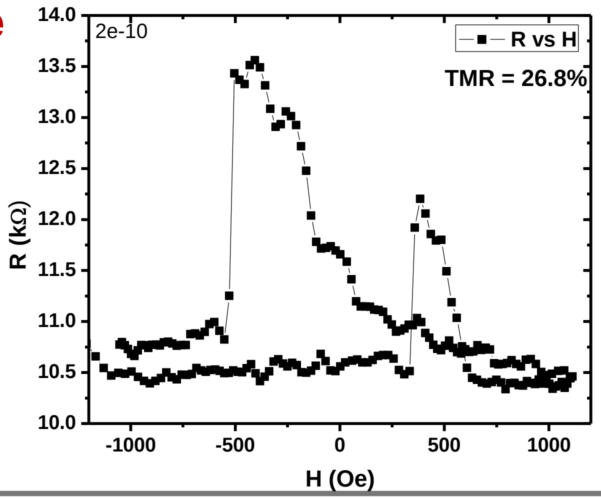

Magnetotransport data (cont.)

LSMO (30)/STO(3)/CFO(3)/Au(100)

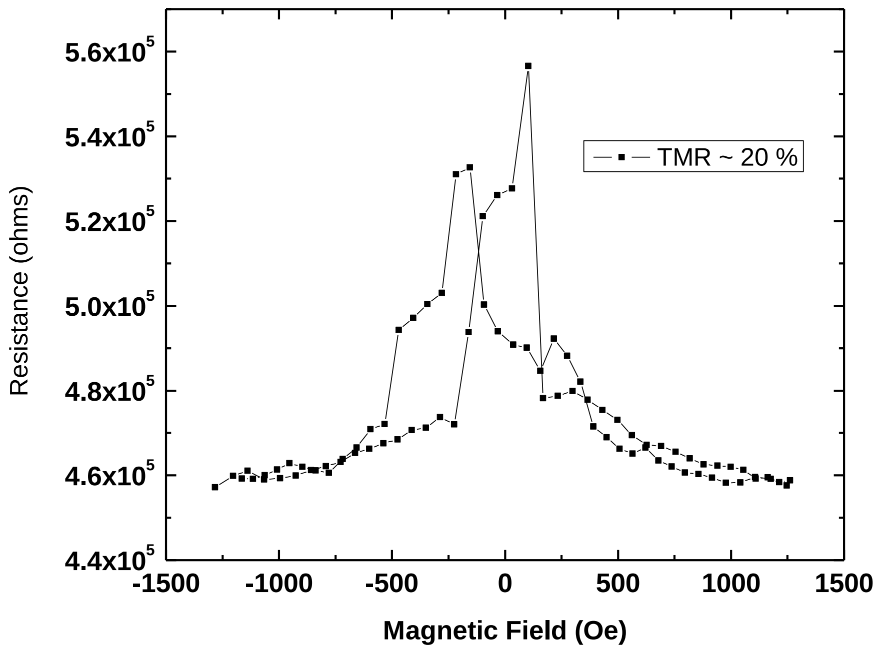

Experimental achievements of past year

- Growth of high quality , atomically flat NFO and CFO thin film achieved over a wide temperature window
- Raman spectroscopy show films grown at higher temperature are single crystal quality
- TEM analysis show presence of anti-phase boundaries
- Cathodoluminescence spectroscopy technique measured a band gap of 3.3eV for NFO films
- Spin filter device prototypes show expected magnetotransport properties

Theoretical – Density Functional techniques

Master equation

$$\left(-\frac{\hbar^2}{2m_e}\Delta + V^{\text{ion}}(\mathbf{r}) + V^{\text{el}}(\mathbf{r}) + V^{\text{xc}}(\mathbf{r})\right)\phi_n(\mathbf{r}) = E_n\phi_n(\mathbf{r})$$

V^{xc}(r) - Exchange and correlation term – Approximated by LDA or GGA in DFT

- **This approach is quite successful in predicting structural properties**
- **Fails to describe excited states – band gap for instance**

Theoretical (cont.) – Hybrid functionals

- Hartree Fock theory → hybrid functionals

$$\left(-\frac{\hbar^2}{2m_e}\Delta + V^{\mathrm{ion}}(\mathbf{r}) + V^{\mathrm{el}}(\mathbf{r})\right)\phi_n(\mathbf{r}) + \int V^{\mathrm{x}}(\mathbf{r},\mathbf{r}')\phi_n(\mathbf{r}')d^3\mathbf{r}' = E_n\phi_n(\mathbf{r})$$

- **Hybrid functional (HF) calculations combine the typical DFT exchange-correlation approximation with a portion of the exact Hartree-Fock exchange. Doing so greatly increases both the accuracy of the band gaps and the time required to run the calculation.**

- **The HSE03 method uses 25% of the exact Hartree-Fock exchange, 75% of the PBE exchange (and 100% of the PBE correlation term), and a screening of the non-local contributions at 0.3 Å.**

Package used -VASP 5.2

Theoretical (cont.)

	PBE	HSE ω=0.300	HSE ω=0.207	PBE0	Expt.
GaAs					
Γ_{1c}	0.56	1.30	1.45	2.01	1.52[a]
X_{1c}	1.46	1.88	2.02	2.67	1.90[a]
L_{1c}	1.02	1.61	1.76	2.37	1.74[a]
Si					
Γ_{15c}	2.57	3.16	3.32	3.97	3.34–3.36,[b] 3.05[c]
X_{1c}	0.71	1.14	1.29	1.93	1.13[d],1.25[c]
L_{1c}	1.54	2.08	2.24	2.88	2.06(3)[e], 2.40(15)[f]
C					
Γ_{15}	5.59	6.74	6.97	7.69	7.3[a]
X_{1c}	4.76	5.68	5.91	6.66	
L_{1c}	8.46	9.77	10.02	10.77	
MgO					
Γ_{15}	4.75	6.24	6.50	7.24	7.7[g]
$X_{4'}$	9.15	10.66	10.92	11.67	
L_1	7.91	9.39	9.64	10.38	
NaCl					
Γ_{15}	5.20	6.31	6.55	7.26	8.5[h]
$X_{4'}$	7.60	8.70	8.95	9.66	
L_1	7.32	8.43	8.67	9.41	
Ar					
Γ_{15}	8.68	10.07	10.34	11.09	14.2[i]

THE JOURNAL OF CHEMICAL PHYSICS 125, 249901 2006

Preliminary Band gap data

Up Spin

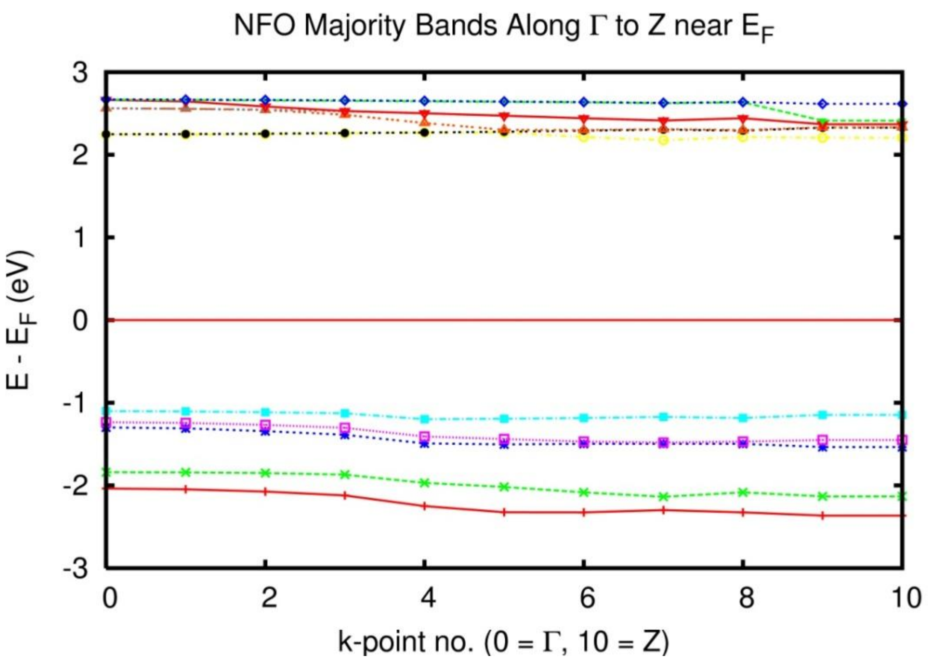

Down Spin

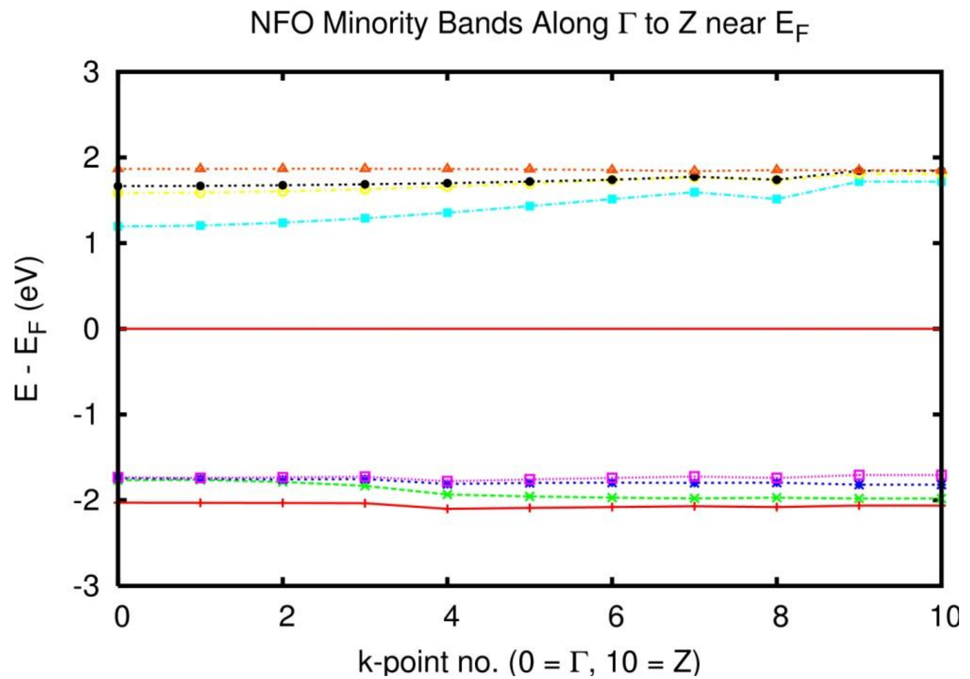

Up spin band gap ~ 3.3 eV

Down spin band gap ~ 3.0 eV

Reasonable agreement with CL data

Future plans

Fundamental issues

1) Address APB issue through growth engineering

2) Spin polarization measurements with TiN and NbTiN.

3) Conducing AFM measurements to extract tunnel barrier properties (barrier height)

4) *Ab-initio* Hybrid functional and GW measurements plus estimate to estimate band gap and exchange splitting . Estimate of decay constant

Devices

1) Working spin-filter demonstration

2) Preliminary double barrier synthesis and TMR properties

Thank you for your attention!!